

## PROTON–NUCLEUS INELASTIC CROSS SECTION AT ULTRAHIGH ENERGY

*T. Kodama*<sup>a</sup>, *L. Portugal*<sup>b</sup>

<sup>a</sup> Instituto de Física, Universidade Federal do Rio de Janeiro, Brazil

<sup>b</sup> Instituto de Física, Universidade Federal Fluminense, Brazil

Energy dependence of proton–nucleus reaction cross section at very high energy is discussed. It is stressed that depending on the gluon distribution near the nuclear surface, proton–nucleus total cross section increases much more rapidly compared to the usual Glauber independent nucleon estimate. The recent observation of  $X_{\max}$  smaller than the expected value at UHECR domain can be an indication for such a mechanism.

PACS: 25.40.-h

### INTRODUCTION

The basic reason why the total or inelastic proton–proton collision cross section increases as a function of the incident energy is that the number of gluons increases in small- $x$  domain. A simple way to see this is as follows.

In the impact parameter representation, the reaction cross section can be expressed as

$$\sigma_r = \int d^2\mathbf{b} [1 - \exp(-2\chi(\mathbf{b}, s))], \quad (1)$$

where the eikonal  $\chi(\mathbf{b}, s)$  counts essentially the total number of possible scattering centers of the constituents inside the target «seen» by the projectile passing through the target along a straight line with the impact parameter  $\mathbf{b}$ , and with center-of-mass energy  $\sqrt{s}$ .

If the target is thick enough, the eikonal function is much larger than unity ( $\chi(\mathbf{b}, s) \gg 1$ ) in the central region, but it falls down to zero in the surface region. The integrand of Eq.(1) keeps a value almost equal to unity while  $\chi(\mathbf{b}, s) \gg 1$ , and falls down quickly to zero near the surface. From this we may determine an effective radius  $b_{1/2}$  such that the integral (1) is approximately given by  $\sigma_r \simeq \pi b_{1/2}^2$ . We may estimate  $b_{1/2}$  by fixing the value of  $\chi(\mathbf{b}_{1/2}, s)$ , for example, as  $\chi(\mathbf{b}_{1/2}, s) = \ln 2$ , so that the effective radius depends on the energy  $b_{1/2} = b_{1/2}(\sqrt{s})$ .

Now let us assume that the eikonal function factorizes in the form  $\chi(\mathbf{b}, s) = P(\mathbf{b})N(\sqrt{s})$ , where  $P(\mathbf{b})$  is the probability distribution of the scattering center (e.g., partons) in the transverse plane, and  $N(x)$  is the number of partons which can interact for a given  $\sqrt{s}$ . Suppose that  $P(\mathbf{b})$  is a two-dimensional Gaussian distribution of width  $R$ ,  $P(\mathbf{b}) \simeq \exp\left\{-\frac{(b/R)^2}{2}\right\}$  and that, for large  $\sqrt{s}$ , the number of partons increases with  $\sqrt{s}$  as  $N(x) \propto \sqrt{s}^\alpha$ . Then, we have

$$b_{1/2}^2(\sqrt{s}) = \alpha R^2 \ln \sqrt{s} + \text{const.} \quad (2)$$

In such a situation, the reaction cross section increases as a function of the incident energy for very large  $\sqrt{s}$  as  $\sigma_r \simeq \alpha\pi R^2 \ln \sqrt{s}$ .

If the edge of the distribution has an exponential tail as  $P(\mathbf{b}) \simeq \exp\{-b/R\}$  instead of a Gaussian distribution, a similar argument will show that the cross section would increase as  $\sigma_r \simeq \text{const} \times (\ln \sqrt{s})^2$ .

The important point of the above simple argument is that the rate of increase is related to the diffuseness  $R$  of the probability distribution of the scattering center. The more diffuse the surface thickness is, the more quickly the reaction cross section increases as a function of the incident energy. The possibility of such a mechanism, not only in the proton–proton but also in nucleus–nucleus cross section, was suggested many years ago [1].

Here we explore the idea of [1] in the language of the QCD gluon saturation mechanism for the proton–nucleus reaction. We show that, if the gluon distribution becomes saturated at some energy scale inside the nuclear surface region, then the reaction cross section of proton–nucleus collisions starts to increase very quickly and eventually overcomes the values estimated by the usual Glauber type of calculation [2].

Applying a simple effective dipole model for the reaction mechanism, we find that such an energy scale is of the order of  $10^{17}–10^{18}$  eV. Above this energy scale, the behavior of the proton–nucleus cross section begins to change. We suggest that such an energy dependence of the proton–nucleus cross section may be observed in terms of the quantity called  $\langle X_{\text{max}} \rangle$  in the air showers of ultrahigh-energy cosmic rays. Using a very simple toy model estimate of  $\langle X_{\text{max}} \rangle$ , we show that our calculated values of the proton–nucleus reaction cross section are consistent with the recently observed  $\langle X_{\text{max}} \rangle$  by the Pierre Auger Observatory experiments [3] for incident protons at ultrahigh energies.

## 1. EFFECTIVE DIPOLE MODEL FOR THE PROTON–PROTON CROSS SECTION

To explore the above idea, we need the total proton–proton cross section as a function of incident energy which permits one to extrapolate to the ultrahigh energy region. For this purpose, we introduce an extremely simplified version of the dipole saturation model for the purpose of illustrating our idea here. The original dipole model was first introduced by Mueller [4] and extended to the impact parameter representation by Kowalski and Teaney [5]. Here, for simplicity, we assume that the proton is described by an effective dipole of a given size  $R_D$ , where we fix the dipole size  $R_D$  by the average dipole radius. In this case, the eikonal for the proton–proton reaction can be written as  $\chi(\mathbf{b}, s) = \pi^2/N_c R_D^2 \alpha_s(Q^2) xg(x, Q^2) T_p(\mathbf{b})$ . Here, the quantity  $xg(x, Q^2)$  is the parton distribution function (PDF), and represents the gluon density  $x$  distribution in the target at a scale  $Q^2$ , and  $\alpha_s(Q^2)$  is the strong coupling defined at this scale. Naturally, our simple effective dipole description will not work well for the low-energy region. However, the objective of the present work is to show the effect of possible gluon saturation inside the nuclear surface region at high energies, we just readjust slightly the parameters determined in [5] to fit the energy dependence of the proton–proton reaction cross section [6] only for  $\sqrt{s} > 100$  GeV. Note that the cross sections for  $\sqrt{s} \simeq 40$  TeV are from the cosmic ray data extracted from the proton–light nuclei interactions. We can obtain reasonable fits using both Gaussian and hyperbolic-secant profile functions at higher

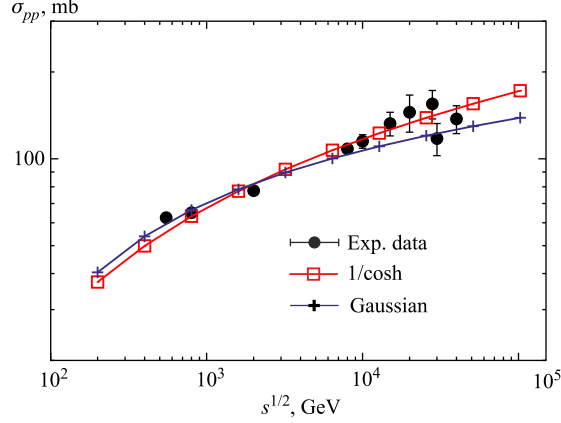


Fig. 1. Fits to proton–proton cross sections. Circles are experimental data [6], crosses are the Gaussian profile function and the open squares are for the hyperbolic secant function

energies, as seen in Fig. 1 [2]. For these calculations we have used the PDF  $xg(x, Q^2)$  from the GRV98 Collaboration [7].

## 2. PROTON–NUCLEUS CROSS SECTION

For a high energy proton–nucleus collision, we may calculate the reaction cross section  $\sigma_{p+A}$  as a superposition of independent nucleon–nucleon collisions in the Glauber approach. Hereafter, this picture is referred to as INGP. In this picture, the eikonal in Eq. (1) is given by the well-known Glauber multiple scattering formula  $\chi_{p+A}^{\text{Glauber}} = A \int_{-\infty}^{\infty} dz P_A(\mathbf{b}, z) \sigma_{pp}(\sqrt{s})$ , where  $\sigma_{pp}(\sqrt{s})$  is the total cross section of the proton–proton collision. Since  $\sigma_{pp}(\sqrt{s}) \simeq \ln(\sqrt{s})$  (or  $\ln^2(\sqrt{s})$ ), we conclude that the INGP leads to a very weak energy dependence of the cross section  $\langle \sigma_{p+A} \rangle \sim \ln \ln(\sqrt{s})$  for large  $\sqrt{s}$ , and the Glauber multiple scattering eikonal leads essentially to the geometric cross section of order  $\pi R_N^2$  plus a slow energy increase.

In contrast to the approach above, we may consider the proton–nucleus collision process in terms of the gluon distribution inside the whole nucleus. When we go to sufficiently large energies, gluons of bounded nucleons inside a nucleus should start to superimpose and eventually fill up the nucleus as a whole. In this regime, we should then use the dipole model with gluon distribution inside the nucleus to calculate the total cross section for proton–nucleus collision. Hereafter, such a scenario is referred to as GSNS. In this case, the eikonal is again given by  $\chi(\mathbf{b}, s) = \pi^2 / N_c R_D^2 \alpha_s(Q^2) xg(x, Q^2) T_N(\mathbf{b})$ , where now  $T_N(\mathbf{b})$  is the transverse probability distribution function of gluons inside the target nucleus. In this regime, as we discussed before, the total reaction cross section increases as  $\ln(\sqrt{s})$  or  $\ln(s)^2$ , depending on the form of gluon profile function near the nuclear surface which is much quicker than  $\ln \ln(\sqrt{s})$  of the independent nucleon picture. Therefore, the total cross

section for proton–nucleus is eventually dominated by the gluon saturation process in the nuclear surface domain.

### 3. A TOY-MODEL ESTIMATE OF $X_{\max}$ IN UHECR DOMAIN

To see in practice what is the crossover energy scale for the gluon saturation inside a nucleus, we compare the calculated total reaction cross sections using the INGP and the GNSN visions. We take typical air nuclei of average  $\langle A \rangle = 14.5$  where  $R_N = 1.1A^{1/3}$  fm. In Fig. 2 we compare the energy dependences of proton–air collision cross sections calculated for various situations: one in the INGP ( $\bullet$ ), and other 3 cases of the GNSN with Gaussian nuclear profile ( $+$ ), GNSN with hyperbolic secant profile ( $\times$ ) and the  $z$ -integrated Woods–Saxon profile ( $\square$ ). The INGP gives almost the same cross section for all the profile functions so that only one line is shown.

As expected, the GNSN scenario gives a rapid increase of the proton–nucleus cross section as a function of the incident energy and eventually overcomes the value of the INGP. It is interesting to note that all of the cross sections for different profile functions of GNSN cross the INGP estimates at the energy scale of  $10^{17}$ – $10^{18}$  eV [2].

One direct consequence of such effects should reflect in the behavior of the observable  $\langle X_{\max} \rangle$ , essentially the normalized depth of the position of maximum luminosity of an air-shower in the atmosphere. This observable can be affected both by the proper increase of the  $p$ – $p$  cross section at ultrahigh energy (as in the case of the  $1/\cosh$  profile) and also by the increase of the  $p$ – $A$  cross section, due to the gluon saturation inside the target nucleus. Another possibility is that the primary particle is not a proton but a heavy nucleus. We concentrate on the second possibility.

To calculate a realistic value of  $\langle X_{\max} \rangle$  we need a sophisticated simulation of the air-shower processes [8] involving all the exclusive cross sections. Here, just to get an idea on how the above increase of the cross section affects  $\langle X_{\max} \rangle$ , we apply a simple toy model due to Heitler [9] to estimate the deviation of  $\langle X_{\max} \rangle$  from these calculations which are based

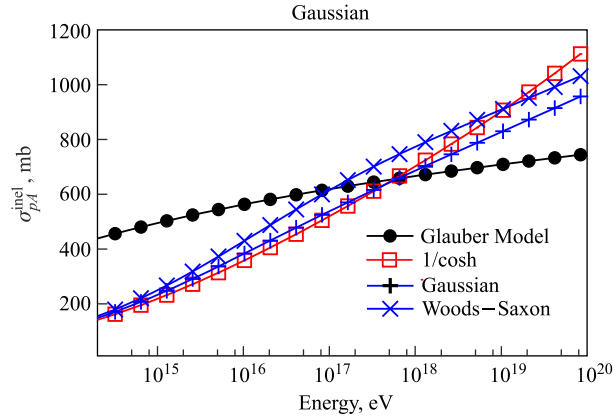


Fig. 2. Proton–nucleus cross sections. Black circles are for the INGP, and other three ( $+$ ,  $\times$ ,  $\square$ ) correspond to the scenario of GNSN

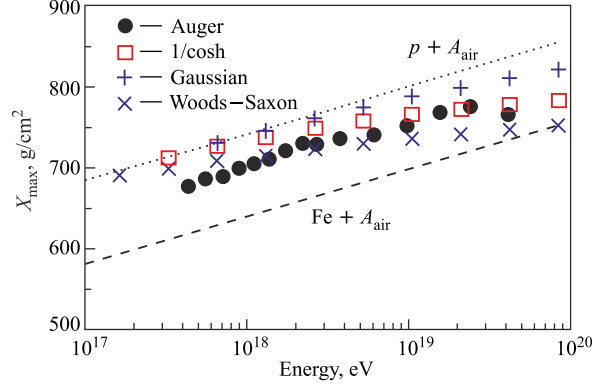


Fig. 3. Estimated  $\langle X_{\max} \rangle$  using the Heitler model. The dotted (proton–air) and dashed (Fe–air) lines are taken from SIBYLL Collaborations [10], and black circles are the observed values extracted from the Auger Experiment. Our  $\langle X_{\max} \rangle$  are calculated for three different profile functions (+ — Gaussian,  $\square$  —  $1/\cosh$ ,  $\times$  — Woods–Saxon) as the deviation from the upper line

on the Glauber description. Assuming that such differences of  $\langle X_{\max} \rangle$  can be identified with the sum of differences of mean free paths calculated from the INGP and the GSNS scenario, we show in Fig. 3 the estimated  $\langle X_{\max} \rangle$  values for three different profile functions (+ — Gaussian,  $\square$  —  $1/\cosh$ ,  $\times$  — Woods–Saxon) together with the SIBYLL calculations [10] for the proton–air and Fe–air simulations (dashed lines) and also the observed values extracted from the Pierre Auger Observatory experiment (black circles).

#### 4. DISCUSSION

In this work, we have shown that if we use the gluon distribution function in the surface region of the target nucleus similar to that of a proton, the proton–nucleus cross section starts to increase more rapidly as a function of the incident energy than that calculated by the Glauber independent nucleon distribution model. In the former, the cross section increases as  $\ln s$  whereas in the later, increases as  $\ln(\ln s)$ . As we see, the difference between the two pictures, INGP and GSNS, becomes very large at high energies. The reason for this is that, while in the INGP the effect of virtual gluons which bound the nucleon near the surface area is completely neglected, these gluons become dominant at high energies in the GSNS scenario.

In a simple-minded argument, one might think that such an effect of nuclear binding must be negligible at high energies, since the ratio of the binding energy of a nucleon to the incident energy tends to zero. However, the situation may not be so simple. In the GSNS scenario, the density of virtual gluons, probably forming a kind of fractal fingers when penetrating into the vacuum among nucleons similar to the electric discharge pattern, becomes large at high energies, and eventually percolate everywhere even in the nuclear surface region. According to the color glass condensate picture [11], such a scenario should happen at some energy scale, even at the lowest density region of the nuclear surface. In the case of proton–proton case, this is exactly the physical mechanism to understand the energy dependence of the cross

section. That is, very peripheral gluons of a nucleon become dense enough to demonstrate a classical field behavior at high energies and contribute to the reaction process. Therefore, we expect GSNS mechanism should eventually happen for an ultrahigh energy scale.

The energy scale and the intensity of the GSNS scenario are determined by the form of the distribution of gluons near the surface area. If we assume that the small- $x$  gluon distribution in the nucleus follows that of the nucleon wave function inside the nucleus, the energy scale where the gluon saturation scenario starts to dominate, the independent nucleon picture is around  $10^{17}$ – $10^{18}$  eV. We note that different profile functions give more or less the same energy scale once the proton–proton cross section is well fitted. It is very suggestive that the gluon saturation scenario inside the surface area seems consistent with the proton primary interpretation of the observed  $\langle X_{\max} \rangle$  behavior in the Pierre Auger Laboratory experiment.

Naturally, the energy scale depends on the precise form of the geometric gluon distribution inside the nucleus. If the distribution does not follow the probability distribution of nucleons but more sharp surface distribution, or very scarce fractal-like structure due to some confinement mechanism, then the energy scale may shift to higher energy. Depending on this, the energy scale can be even lower than estimated here. To find a real energy scale where the gluon saturation occurs at the nuclear surface, further investigation on high–energy proton–nucleus or electron–nucleus collisions will be necessary.

This work has been supported by FAPERJ, CAPES, CNPq, and PRONEX. The authors thank Larry McLerran, C.E. Aguiar, and E. Fraga for fruitful discussions and for encouragement.

#### REFERENCES

1. Kodama T. *et al.* // Nucl. Phys. A. 1991. V. 523. P. 640–650;  
Barroso M. F., Kodama T., Hama Y. // Phys. Rev. C. 1996. V. 53. P. 501–504.
2. Portugal L., Kodama T. // Nucl. Phys. A. 2010. V. 837. P. 1–14.
3. Unger M. (*The Pierre Auger Collab.*) // Proc of the 30th Intern. Cosmic Ray Conf., Merida, 2007. V. 4. P. 373–376; arXiv:astro-ph/0706.1495.
4. Mueller A. H. // Nucl. Phys. B. 1990. V. 335. P. 115–137.
5. Kowalski H., Teaney D. // Phys. Rev. D. 2003. V. 68. P. 114005; arXiv:hep-ph/0304189;  
Further developments are found in Kowalski H., Lappi T., Venugopalan R. // Phys. Rev. Lett. 2008. V. 100. P. 022303; arXiv:hep-ph/0705.3047;  
Kowalski H. *et al.* // Phys. Rev. C. 2008. V. 78. P. 045201; arXiv:hep-ph/0805.4071;  
Bartels J., Golec-Biernat K. J., Kowalski H. // Phys. Rev. D. 2002. V. 66. P. 014001; arXiv:hep-ph/0203258;  
Bartels J. *et al.* // Phys. Lett. B. 2003. V. 556. P. 114–122; arXiv:hep-ph/0212284.
6. Avila C. *et al.* (*E-811 Collab.*) // Phys. Lett. B. 2002. V. 537. P. 41–44;  
Abe F. *et al.* (*CDF Collab.*) // Phys. Rev. D. 1994. V. 50. P. 5550–5561;  
Amos N. A. *et al.* (*E710 Collab.*) // Phys. Rev. Lett. 1992. V. 68. P. 2433–2436;  
Honda M. *et al.* // Phys. Rev. Lett. 1993. V. 70. P. 525–528;  
Baltrusaitis R. M. *et al.* // Phys. Rev. Lett. 1984. V. 52. P. 1380–1383.
7. Gluck M., Reya E., Vogt A. // Eur. Phys. J. C. 1998. V. 5. P. 461–470; arXiv:hep-ph/9806404.
8. Bossard G. *et al.* // Phys. Rev. D. 2001. V. 63. P. 054030; arXiv:hep-ph/0009119;  
Drescher H. J., Farrar G. R. // Phys. Rev. D. 2003. V. 67. P. 116001; arXiv:astro-ph/0212018;  
Heck D. *et al.* Report. 1998. FZKA 6019.

9. *Gaisser T. K.* Cosmic Rays and Particle Physics. Cambridge, UK: Cambridge Univ. Press, 1990. P. 201–202.
10. *Fletcher R. S. et al.* // Phys. Rev. D. 1994. V. 50. P. 5710–5731.
11. *McLerran L. D., Venugopalan R.* // Ibid. V. 49. P. 2233–2241; arXiv:hep-ph/9309289;  
*Iancu E., Leonidov A., McLerran L. D.* // Nucl. Phys. A. 2001. V. 692. P. 583–645; arXiv:hep-ph/0011241;  
*Iancu E., McLerran L. D.* // Phys. Lett. B. 2001. V. 510. P. 145–154; arXiv:hep-ph/0103032;  
*Jalilian-Marian J. et al.* // Phys. Rev. D. 1997. V. 55. P. 5414–5428; arXiv:hep-ph/9606337.